Numb deficiency in cerebellar Purkinje cells impairs synaptic expression of metabotropic glutamate receptor and motor coordination

Liang Zhou[a,1], Dong Yang[a,1], De-Juan Wang[a,1], Ya-Jun Xie[a], Jia-Huan Zhou[a], Lin Zhou[a], Hao Huang[b], Shuo Han[a], Chong-Yu Shao[a], Hua-Shun Li[c], J. Julius Zhu[d], Meng-Sheng Qiu[b], Chris I. De Zeeuw[e,f,2], and Ying Shen[a,2]

[a]Department of Neurobiology, Key Laboratory of Medical Neurobiology of Ministry of Health, Zhejiang University School of Medicine, Hangzhou 310058, China; [b]Institute of Developmental and Regenerative Biology, College of Life and Environmental Science, Hangzhou Normal University, Hangzhou 310029, China; [c]SARITEX Center for Stem Cell Engineering Translational Medicine, Shanghai East Hospital, Tongji University School of Medicine, Shanghai 200123, China; [d]Department of Pharmacology, School of Medicine, University of Virginia, Charlottesville, VA 22908; [e]Department of Neuroscience, Erasmus University Medical Center, 3000 CA, Rotterdam, The Netherlands; and [f]Netherlands Institute for Neuroscience, Royal Dutch Academy for Arts and Sciences, Meibergdreef 47, Amsterdam, The Netherlands

Edited by Richard L. Huganir, The Johns Hopkins University School of Medicine, Baltimore, MD, and approved November 13, 2015 (received for review July 2, 2015)

Protein Numb, first identified as a cell-fate determinant in *Drosophila*, has been shown to promote the development of neurites in mammals and to be cotransported with endocytic receptors in clathrin-coated vesicles in vitro. Nevertheless, its function in mature neurons has not yet been elucidated. Here we show that cerebellar Purkinje cells (PCs) express high levels of Numb during adulthood and that conditional deletion of Numb in PCs is sufficient to impair motor coordination despite maintenance of a normal cerebellar cytoarchitecture. Numb proved to be critical for internalization and recycling of metabotropic glutamate 1 receptor (mGlu1) in PCs. A significant decrease of mGlu1 and an inhibition of long-term depression at the parallel fiber–PC synapse were observed in conditional Numb knockout mice. Indeed, the trafficking of mGlu1 induced by agonists was inhibited significantly in these mutants, but the expression of ionotropic glutamate receptor subunits and of mGlu1-associated proteins was not affected by the loss of Numb. Moreover, transient and persistent forms of mGlu1 plasticity were robustly induced in mutant PCs, suggesting that they do not require mGlu1 trafficking. Together, our data demonstrate that Numb is a regulator for constitutive expression and dynamic transport of mGlu1.

Numb | mGlu1 | trafficking | Purkinje cell | cerebellum

Numb was first identified in *Drosophila melanogaster* (1) and is evolutionarily conserved across species (2). During cell division it segregates asymmetrically in dividing cells and determines cell fate by interacting with and inhibiting Notch (2–4). Numb and Numblike, two homologs in mammals (5), are believed to play redundant roles (6). Numb contains a phosphotyrosine-binding domain (PTB), a proline-rich domain (PRR), and two Eps15 homology regions (DPF and NPF). These domains and motifs make Numb an adaptor protein capable of interacting with a number of molecules including Notch, Hedgehog, and p53 (2).

In the mammalian CNS Numb/Numblike is essential for maintaining neural stem cells during neurogenesis (7–10). Numb may play a critical role in axonal growth during the development of hippocampal pyramidal cells by mediating endocytosis of neuronal adhesion molecule L1 (11), and knocking down Numb/Numblike reduces spine density (12). Numb/Numblike is expressed not only in neuronal progenitor cells but also in postmitotic adult neurons (5); however, in mature neurons the cellular function of Numb and its role at the system level in vivo are unknown.

Because Numb is located in clathrin-coated vesicles and is cotransported with endocytic receptors (13), we hypothesized that in adult mammals it might be involved in long-term plasticity and trafficking of glutamate receptors (14). We used cerebellar Purkinje cells (PCs) as a model system to investigate these processes, because these associations have been clearly laid out in PCs, and they may reveal tractable read-outs at the behavioral level (15–18). Our data indicate that conditional deletion of Numb in PCs causes functional deficits in motor coordination, which may be ascribed to reduced trafficking of metabotropic glutamate 1 receptor (mGlu1) to perisynaptic sites at parallel fiber (PF)–PC synapses.

Results

Adult PCs Express Numb but Not Numblike. Expression of Numb was fairly weak in mice at birth but increased to a peak at approximately postnatal day (P)10 and remained constant thereafter (Fig. 1*A* and Fig. S1). The mRNA expressions of *Numb* and its close homolog *Numblike* (5) were examined in whole cerebella and individual PC somata using RT-PCR (19–21). Transcripts of both were detected in the whole cerebellum of P30 mice, but only *Numb* was found in PCs (Fig. 1*B*). The transcription patterns of *Numb* and *Numblike* also were examined with in situ hybridization of P30 mice. In accord with RT-PCR, *Numb* hybridization was localized to PC somata, but no signal for *Numblike* was found (Fig. 1*C*). The exclusive expression of *Numb* in P30 PCs was unexpected, because Numb and Numblike had been found to coexist in neuronal precursor cells (22).

Significance

Protein Numb controls cell fate by interacting with a number of signaling molecules, critical for maintaining neural stem cells and neuronal development in the central nervous system. However, the function of Numb has not been studied in mature neurons. Here, we found that deletion of Numb in cerebellar Purkinje cells causes deficits in motor learning, which can be ascribed to a reduced level of synaptic metabotropic glutamate 1 receptor (mGlu1). Although Numb deficiency does not alter the expression of mGlu1-associated proteins and activity-dependent plasticity of mGlu1, it inhibits intracellular trafficking of mGlu1. To our knowledge, our work is the first to demonstrate an important function of Numb in mature neurons.

Author contributions: Liang Zhou, D.Y., D.-J.W., and Y.S. designed research; Liang Zhou, D.Y., D.-J.W., Y.-J.X., J.-H.Z., Lin Zhou, H.H., S.H., and C.-Y.S. performed research; H.-S.L., J.J.Z., M.-S.Q., and C.I.D.Z. contributed new reagents/analytic tools; Liang Zhou, D.Y., D.-J.W., Y.-J.X., J.-H.Z., M.-S.Q., and Y.S. analyzed data; and J.J.Z., C.I.D.Z., and Y.S. wrote the paper.

The authors declare no conflict of interest.

This article is a PNAS Direct Submission.

[1]Liang Zhou, D.Y., and D.-J.W. contributed equally to this work.

[2]To whom correspondence may be addressed. Email: yshen@zju.edu.cn or c.dezeeuw@erasmusmc.nl.

This article contains supporting information online at www.pnas.org/lookup/suppl/doi:10.1073/pnas.1512915112/-/DCSupplemental.

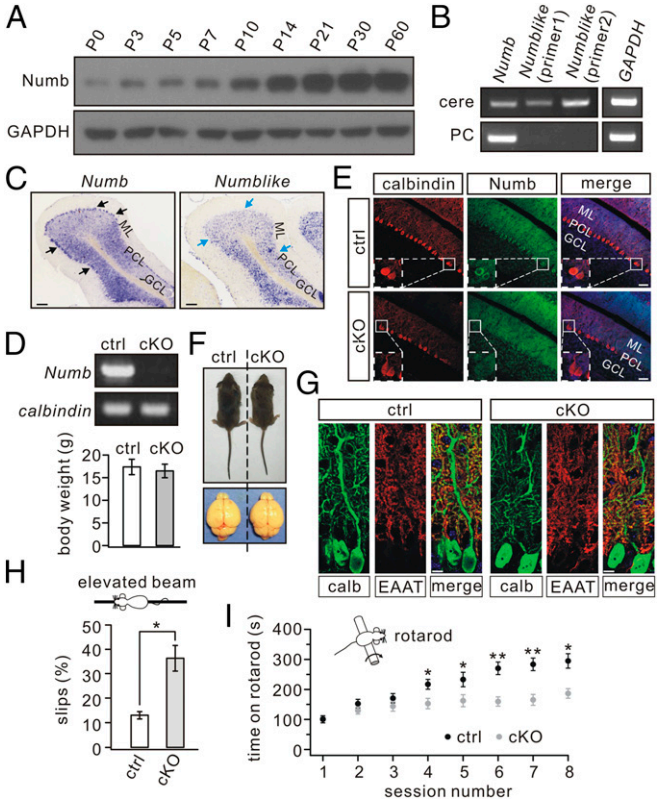

Fig. 1. Impaired motor coordination in Numb-cKO mice. (*A*) Numb expression at different postnatal stages in control cerebellum. *GAPDH* was the internal control. (*B*) Electrophoresis of *Numb* (214 bp), *Numblike* (369 bp), and *GAPDH* (172 bp) amplicons from cerebellar extracts (cere) ($n = 5$) and individual PCs ($n = 7$). (*C*) In situ hybridization with *Numb* and *Numblike* riboprobes in cerebellar sagittal sections from P30 control mice ($n = 5$). Note that *Numb* (black arrows), but not *Numblike* (blue arrows), was expressed abundantly in PCs. GCL, granule cell layer; ML, molecular layer; PCL, PC layer. (Scale bars: 100 μm.) (*D*) Electrophoresis of *Numb* and *calbindin* from individual control and Numb-cKO PCs ($n = 10$). (*E*) Immunohistochemical staining for calbindin (red), Numb (green), and DAPI (blue) in the cerebellum from control and Numb-cKO mice. Higher magnifications in dashed white boxes indicate that Numb signal is absent from Numb-cKO PCs. (Scale bars: 50 μm.) (*F*) Numb-cKO mice (P21) displayed normal body size and brain. Average body weights were 17.5 ± 1.7 g (control) and 16.6 ± 1.5 g (cKO) ($n = 12$ pairs; $P > 0.05$). (*G*) Immunostaining for calbindin (calb, red) and EAAT4 (green) shows dendrites and spine formation are normal in Numb-cKO mice compared with control. (Scale bars: 10 μm.) (*H*) Percentage of steps with hindpaw slips during runs on an elevated horizontal beam ($n = 10$ pairs). (*I*) Time spent on the accelerating rotarod for control and Numb-cKO mice ($n = 10$ pairs). $*P < 0.05$, $**P < 0.01$.

Numb Deficiency in PCs Does Not Impair Cyto-Architecture but Affects Motor Coordination. To assess potential roles of Numb at the system level, we generated conditional knockout (cKO) mice that lacked Numb specifically in PCs using the L7-promoter (Numb-cKO) (23). Deletion of Numb in PCs of Numb-cKO animals was confirmed by a lack of the *Numb* band following RT-PCR of mRNA extracted from their PCs (Fig. 1*D*) and by the lack of immunostaining in their PCs (Fig. 1*E*). The preserved Numb signal in the granular and molecular layers (Fig. 1*E*) is in line with the expression of Numb in granule cells and Bergmann glia, as shown during development (10, 24). Postnatal Numb-cKO mice (P21) appeared normal, as shown by unchanged body weight and cerebellar size (Fig. 1*F*). Also, their cerebellar cyto-architecture appeared normal following immunostaining for calbindin and excitatory amino acid transporter 4 (EAAT4) (25). Moreover, PC-specific Numb deficiency did not interfere with lobule thickness, dendritic branching, or number of spines (Fig. 1 *E* and *G* and Fig. S2).

Numb-cKO mice did not show overt ataxia in standard cages (Movie S1). However, they performed poorly, with a remarkably higher number of hind-paw slips, when walking on a narrow elevated beam (Fig. 1*H*). Numb-cKO mice also exhibited impaired motor learning in that they showed limited improvement after four or five sessions on the accelerating rotarod compared with controls (Fig. 1*I*). Together, these results indicate that Numb deficiency in PCs impairs motor coordination.

Long-Term Depression Is Blocked but Long-Term Potentiation Is Normal in Numb-cKO Mice. Given the location of Numb in clathrin-coated vesicles and the role of clathrin-mediated endocytosis of glutamate receptors in the expression of long-term depression (LTD) (14), we examined LTD at PF–PC synapses in Numb-cKO mice in voltage-clamp mode. As shown by paired-pulse responses to PF stimulation before and after LTD induction (Fig. 2*A*), control PCs showed robust PF-LTD (t = 38 min: 67 ± 7% of baseline; $n = 12$, $P < 0.01$) (Fig. 2*B*) in response to repetitive PF tetanus paired with PC depolarization. However, LTD induced with this protocol was blocked in Numb-cKO PCs (t = 38 min: 93 ± 6% of baseline; $n = 11$, $P > 0.05$) (Fig. 2*B*). Likewise, LTD of PF excitatory postsynaptic potentials (EPSPs) induced by a conjunction of double PF shocks and PC depolarization (200 ms, 1 nA) repeated at 1 Hz for 5 min in current-clamp mode was also blocked in Numb-cKO mice (Fig. S3) (26, 27). The ratio of paired-pulse facilitation (PPF) measured at an interval of 80 ms was not changed after LTD induction in control and Numb-cKO mice (Fig. 2*C*), indicating that presynaptic glutamate release was not affected.

Because not only PF-LTD (18, 28–31), but also PF–long-term potentiation (LTP) (17, 32–34), has been proposed as a potential factor contributing to cerebellar motor learning, we investigated the induction of PF-LTP in Numb-cKO mice using a 1-Hz tetanus protocol according to previous work (35–37). After acquiring stable excitatory postsynaptic currents (EPSCs) under voltage-clamp mode (−70 mV), a tetanus stimulation (1 Hz for 5 min) was delivered to PFs while the PC was current-clamped (Fig. 2*D*). The potentiation of EPSC reached 131 ± 4% of baseline in control mice (t = 38 min; $n = 11$, $P < 0.01$) (Fig. 2*E*). The same protocol in Numb-cKO

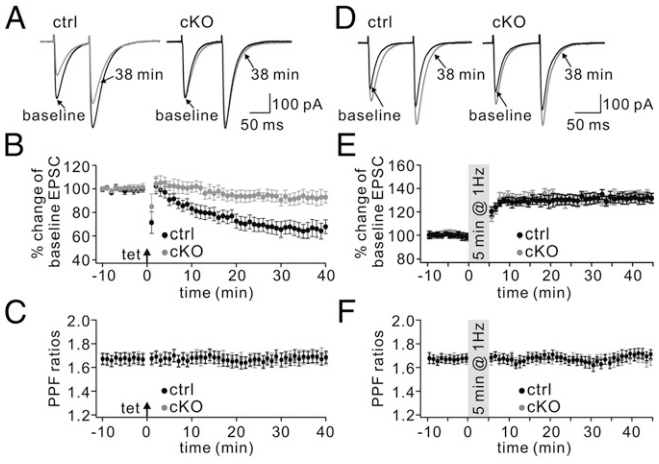

Fig. 2. Inhibited LTD but normal LTP in Numb-cKO mice. (*A*) Two consecutive PF EPSCs before (baseline) and after (t = 38 min) LTD induction in control (ctrl) and Numb-cKO PCs. The interval between paired EPSCs was 80 ms. (*B*) Time courses for percentage changes of EPSC1 amplitude in control (black) and Numb-cKO (gray) mice. Each data point was the average of three successive EPSCs evoked at 0.05 Hz. The arrow indicates LTD induction. (*C*) Time courses for PPF from the cells shown in *B*. (*D*) Example consecutive PF EPSCs before (baseline) and after (t = 38 min) LTP induction. (*E*) Time courses for percentage changes of EPSC1 amplitude in control (black) and Numb-cKO (gray) mice. (*F*) Time courses for PPF ratios from the subset of cells shown in *E*.

mice evoked LTP equally successfully (132 ± 4% at t = 38 min; $n = 10$, $P < 0.01$) (Fig. 2*E*), suggesting that Numb is not associated with PF-LTP. The PPF ratio was unaffected after induction in both control and Numb-cKO mice (Fig. 2*F*), indicating that this LTP is expressed postsynaptically.

mGlu1 Is Reduced at PC Synapses in Numb-cKO Mice. Impaired PF-LTD and motor deficits may result from altered mGlu1 expression (30, 38) and/or glutamatergic transmission (39). Therefore, expression levels of mGlu1 and ionotropic glutamate receptors were examined in relation to those of Numb and calbindin. In control cerebellum (P30) Numb was detected in the isolated synaptic fraction (Fig. 3*A*), in line with previous work (11). In Numb-cKO cerebellum (P30) Numb expression was significantly reduced in both total and synaptic fractions ($P < 0.01$) (Fig. 3*A*); the remaining Numb may have been from cells other than PCs, because Numb was not present in PCs of Numb-cKO mice (Fig. 1 *D* and *E*). The amount of calbindin was similar in control and Numb-cKO mice (Fig. 3*A*), once again indicating that PC development is normal in Numb-cKO mice. Interestingly, synaptic mGlu1 was significantly reduced in Numb-cKO mice ($P < 0.01$), although its total expression was not changed (Fig. 3*A*). Because mGlu1 is highly expressed at excitatory synapses on PCs (30, 40), this result suggests that PC ablation of Numb may directly cause the reduction of mGlu1 at PC synapses. In contrast, neither AMPA receptor (AMPAR) subunit GluA2 nor NMDA receptor (NMDAR) subunit GluN1 was changed in the whole cerebellum or at the synaptic level ($P > 0.05$) (Fig. 3*A*).

If the level of mGlu1 is reduced at PF–PC synapses, we should be able to record a specific difference in currents using whole-cell recordings. Following burst (100 Hz) stimulation of PFs under a holding voltage of −70 mV in artificial cerebrospinal fluid (aCSF) supplemented with 5 μM NBQX (an AMPAR agonist), PCs displayed fast currents mediated by AMPARs and a slow component mediated by mGlu1 (Fig. 3*B*) (41, 42). The peak amplitude of mGlu1 EPSC was reduced significantly in Numb-cKO mice (165 ± 12 pA; $n = 14$) compared with controls (237 ± 18 pA; $n = 14$; $P < 0.01$) (Fig. 3*B*). Moreover, we measured mGlu1 currents evoked by a brief pulse of aCSF containing the mGlu1 agonist 3,5-dihydroxyphenylglycine (DHPG; 100 μM) onto recorded PCs (41). DHPG-induced currents were markedly smaller in Numb-cKO mice (196 ± 12 pA; $n = 13$) than in controls (348 ± 19 pA; $n = 12$; $P < 0.01$) (Fig. 3*C*). Finally, the reduction of mGlu1 currents in Numb-cKO mice was confirmed further when multiple PF stimulations (5 or 15 pulses at 100 Hz) or different doses of DHPG (50 and 150 μM) were applied (Fig. S4). In contrast, AMPA currents were not affected in PCs of Numb-cKO mice, because the time constants of AMPA EPSC decay were not significantly different ($P > 0.05$) (Fig. 3*D*), both frequency and amplitude of AMPA miniature EPSCs (mEPSCs) were unaltered ($P > 0.05$) (Fig. 3*E*) (43), and the PPF of AMPA EPSCs did not change at different stimulus intervals ($P > 0.05$) (Fig. 3 *F* and *G*).

We next investigated whether impaired PF-LTD may be caused by altered endocannabinoid production, P/Q-type Ca^{2+} channels, or climbing fiber (CF) synapse elimination, all of which are involved in PF-LTD (44–46). We found that depolarization-induced suppression of excitatory synapses (DSE), which depends on Ca^{2+}-mediated endocannabinoid production (44, 47–50), was induced normally in Numb-cKO mice (Fig. S5 *A–D*). In addition, PCs can produce endocannabinoid through mGlu1 signaling (51, 52). We found that the inhibition of PF EPSPs induced by high-frequency stimuli (52) did not differ in control and Numb-cKO mice (Fig. S5 *E–H*), suggesting that mGlu1-induced endocannabinoid production is not affected by Numb deficiency. Moreover, there was no difference in P/Q channel-mediated Ca^{2+} transient between control and Numb-cKO mice (Fig. S6). Finally, CF EPSCs were elicited in an all-or-none fashion in the majority of PCs in both control and Numb-cKO mice (Fig. S7), suggesting no difference

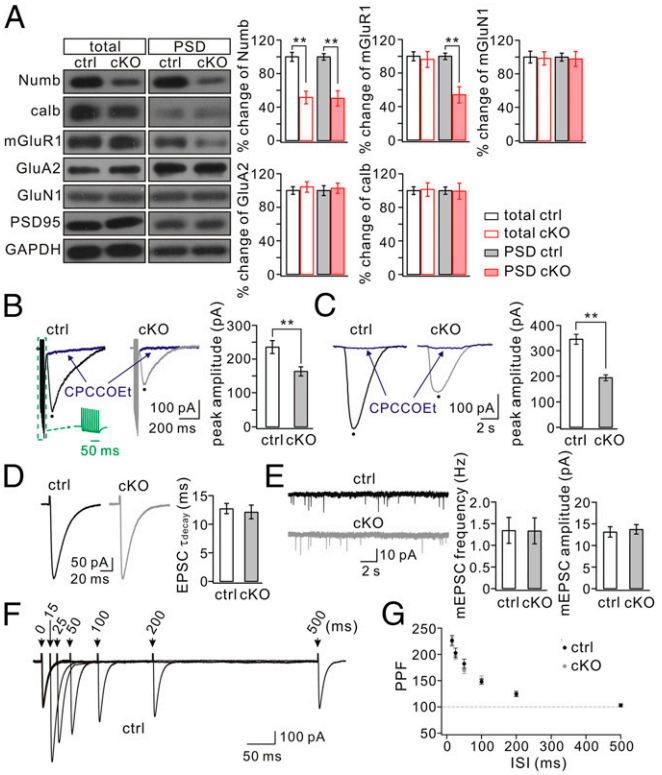

Fig. 3. Synaptic mGlu1 is reduced in Numb-cKO mice. (*A*) Cerebellar (total) and PSD fractions from control (ctrl) and Numb-cKO mice were probed with antibodies to Numb, calbindin, mGlu1, GluA2, and GluN1. GAPDH and PSD95 were internal controls for total and PSD, respectively. Histograms show percentage changes of proteins in Numb-cKO mice relative to control. Control ($n = 4$): 100 ± 5% (total, Numb), 100 ± 4% (PSD, Numb); 100 ± 4% (total, calbindin), 100 ± 4% (PSD, calbindin); 100 ± 5% (total, mGlu1), 100 ± 4% (PSD, mGlu1); 100 ± 4% (total, GluA2), 100 ± 6% (PSD, GluA2); 100 ± 7% (total, GluN1), 100 ± 5% (PSD, GluN1). Numb-cKO ($n = 4$): 51 ± 7% (total, Numb), 50 ± 9% (PSD, Numb); 101 ± 8% (total, calbindin), 99 ± 9% (PSD, calbindin); 96 ± 9% (total, mGlu1), 54 ± 9% (PSD, mGlu1); 104 ± 6% (total, GluA2), 102 ± 6% (PSD, GluA2); 98 ± 8% (total, GluN1), 97 ± 9% (PSD, GluN1). (*B*) mGlu1 EPSCs produced by a PF burst (*Green Inset*: 10 pulses, 100 Hz). mGlu1 EPSCs were blocked by its antagonist CPCCOEt (100 μM). Peaks were measured as indicated by black dots. (*C*) Slow currents were evoked by a pulse (10 psi, 20 ms) of aCSF containing DHPG (100 μM) and were blocked by the mGlu1 antagonist CPCCOEt (100 μM). (*D*) Representative AMPA EPSCs in control and Numb-cKO PCs. The decay was fit with a single exponential in both cells, and mean time-constants were 12.8 ± 0.9 ms (control; $n = 24$) and 12.2 ± 1.2 ms (cKO; $n = 30$). (*E*) mEPSCs recorded from control ($n = 10$) and Numb-cKO ($n = 10$) PCs. mEPSC parameters were frequency, 1.4 ± 0.3 (control) and 1.3 ± 0.3 (cKO); amplitude, 13.2 ± 1.2 pA (control) and 13.8 ± 1.1 pA (cKO). (*F*) Superposition of PF EPSCs evoked at different intervals in a control cell. (*G*) PPF as a function of interstimulus interval in control ($n = 11$) and Numb-cKO ($n = 12$) cells. $^{**}P < 0.01$.

in CF synapse elimination. These results support the notion that endocannabinoid signaling, P/Q-type Ca^{2+} channels, and CF synapse elimination in PCs do not contribute to impaired PF-LTD in Numb-cKO mice. Previous studies have reported that CF elimination is impaired in mGlu1 null-mutant mice (30, 53) but can be partially restored by transgenic expression of mGlu1 (27, 30). Our data extend these findings and suggest that partial preservation of mGlu1 can be sufficient for CF elimination.

Levels of mGlu1-Associated Proteins Are Normal in Numb-cKO Mice. mGlu1 function may depend on associated modifying proteins (19, 54–60). Thus, the cellular changes in mGlu1 expression and currents at PC synapses might reflect a secondary process caused by an ablated interaction between Numb and one or more proteins

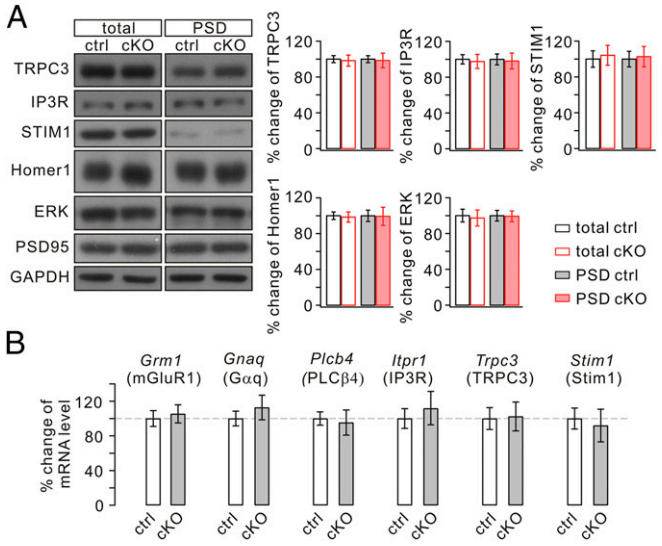

Fig. 4. Expressions of mGlu1-associated proteins are normal in Numb-cKO mice. (*A*) Cerebellar (total) and PSD fraction of control (ctrl) and Numb-cKO mice were probed by immunoblotting with antibodies to TRPC3, IP_3R, STIM1, Homer1, and ERK. GAPDH and PSD95 were loading controls for total and PSD, respectively. Percentage changes of signal intensities were control, 100 ± 4% (total, TRPC3), 100 ± 4% (PSD, TRPC3); 100 ± 5% (total, IP_3R) 100 ± 6% (PSD, IP_3R); 100 ± 8% (total, STIM1), 100 ± 8% (PSD, STIM1); 100 ± 4% (total, Homer1), 100 ± 6% (PSD, Homer1); 100 ± 7% (total, ERK), 100 ± 6% (PSD, ERK); cKO, 98 ± 6% (total, TRPC3), 98 ± 8% (PSD, TRPC3); 96 ± 8% (total, IP_3R), 97 ± 8% (PSD, IP_3R); 104 ± 11% (total, STIM1), 103 ± 11% (PSD, STIM1); 98 ± 5% (total, Homer1), 99 ± 9% (PSD, Homer1); 98 ± 9% (total, ERK), 99 ± 6% (PSD, ERK). $n = 4$. (*B*) Percentage changes of transcript copy numbers per cell for the indicated genes. *Grm1*, 100 ± 9% ($n = 13$, control) and 105 ± 10% ($n = 14$, cKO); *Gnaq*, 100 ± 8% ($n = 13$, control) and 113 ± 14% ($n = 14$, cKO); *Plcb4*, 100 ± 8% ($n = 13$, control) and 95 ± 14% ($n = 14$, cKO); *Itpr1*, 100 ± 11% ($n = 13$, control) and 112 ± 19% ($n = 14$, cKO); *Trpc3*, 100 ± 13% ($n = 13$, control) and 102 ± 17% ($n = 14$, cKO); *Stim1*, 100 ± 12% ($n = 13$, control) and 92 ± 19% ($n = 14$, cKO).

that interact with mGlu1. We therefore investigated the levels of mGlu1-associated substrates in Numb-cKO mice. Western blots showed deletion of Numb in PCs did not affect the total or synaptic level of mGlu1-related proteins (Fig. 4*A*), including transient receptor potential channel 3 (TRPC3) (56, 57), inositol trisphosphate receptor (IP_3R) (55), stromal interaction molecule 1 (STIM1) (58), Homer1 (59), and ERK (60). Furthermore, real-time quantitative RT-PCR was used to detect transcripts of mGlu1 (*Grm1*) and genes of associated proteins [*Gnaq* ($G\alpha_q$) (19), *Plcb4* (PLCβ4) (55), *Itpr1* (IP_3R) (55), *Trpc3* (TRPC3) (56, 57), and *Stim1* (Stim1) (58)] in individual PCs. Numb deficiency in PCs did not interfere significantly with mRNA levels of these genes (Fig. 4*B*). These results suggest that the reduced level of synaptic mGlu1 currents is not caused by deregulation of its associated proteins.

Numb Deficiency Affects mGlu1 Trafficking but Not Its Plasticity. Kim et al. (61) found that mGlu1 currents themselves can exhibit persistent depression (mGluR LTD) following CF stimulation-like depolarization. Because Numb is located in clathrin-coated vesicles and is transported along with endocytic receptors (13), it might be involved in mGlu1 LTD. To address this question, we recorded mGlu1 EPSCs for a stable period and applied a 5-s step depolarization from −70 mV to 0 mV to clamped PCs. In control PCs, mGlu1 EPSCs decreased immediately (30 s after depolarization) and showed a strong depression 30 min later (Fig. 5*A*). The decrease in mGlu1 EPSCs was slower and the final depression was less substantial (t = 30 min: 19 ± 6% of baseline; $n = 12$, $P < 0.01$) (Fig. 5*B*) than reported by Kim et al. (61). Against our assumption, the amplitude of mGlu1 EPSC also was decreased after depolarization in mutant PCs (t = 30 min: 25 ± 7% of baseline; $n = 12$, $P < 0.01$) (Fig. 5 *A* and *B*), showing no difference between controls and mutants ($P > 0.05$). The amplitudes of AMPA EPSCs did not show any change after depolarization either in controls or in Numb-cKO mice ($P > 0.05$) (Fig. 5*B*), consistent with previous work (58). These data suggest that Numb is not directly involved in the induction of mGlu1-LTD.

mGlu1 EPSCs also can undergo a transient (short-term) upregulation (mGlu1-STP) in response to a brief depolarizing current (41, 62), so we next investigated to what extent Numb might be required for mGlu1-STP. After recording a test mGlu1 EPSC, somatic depolarization to 0 mV for 100 ms was delivered to the recorded PC. A second mGlu1 EPSC was evoked at intervals of 10 to 180 s (Fig. 5*C*). The conditioning depolarization produced a potentiation of mGlu1 current but had no effect on AMPA EPSCs ($P > 0.05$) (Fig. 5*D*). We found that mGlu1-STP was induced robustly in both control and Numb-cKO PCs at similar degrees across a range of intervals (Fig. 5*D*), indicating that Numb is not involved in mGlu1-STP.

It has been shown that mGlu1 is internalized (63–66) and recycled back into the cell membrane (65) upon ligand exposure. Because trafficking may affect receptor targeting at the cell membrane, we investigated whether Numb is involved in the internalization and recycling of mGlu1. DHPG (100 μM) was applied to acute cerebellar slices for 10 min, and the level of synaptic mGlu1 was measured 30 min (for endocytosis) or 180 min (for recycling) after DHPG application. In control slices, synaptic

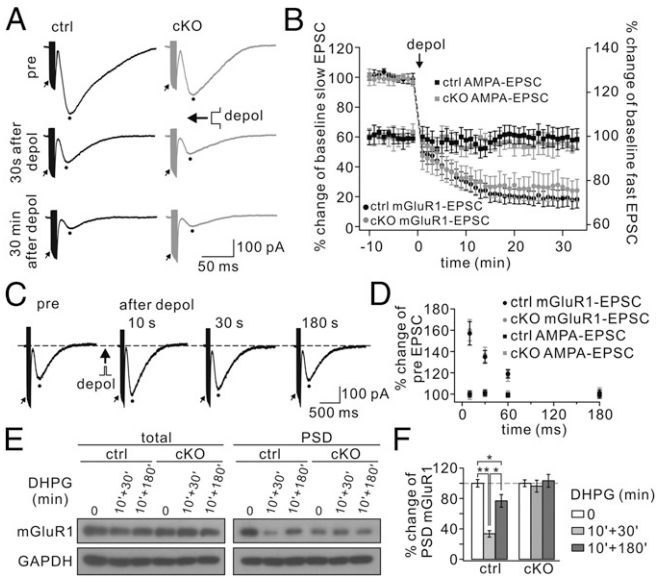

Fig. 5. mGlu1-LTD and mGlu1-STP are normal, but mGlu1 trafficking is inhibited in Numb-cKO mice. (*A*) mGlu1 EPSCs before and after the conditioning depolarization (depol; 5-s command to 0 mV at the soma) in control (ctrl) and Numb-cKO cells. Peaks of mGlu1 EPSCs and first AMPA EPSCs were measured as indicated by dots and arrows, respectively. (*B*) Time courses of percentage changes of mGlu1 EPSCs (left *y* axis) and AMPA EPSCs (right *y* axis) from control ($n = 12$) and Numb-cKO ($n = 12$) cells before and after 5-s depolarization. (*C*) Representative traces from one control PC showing trials before (pre), and 10, 30, and 180 s after somatic depolarization to 0 mV for 100 ms. (*D*) Time courses for percentage changes of mGlu1 EPSCs and AMPA EPSCs in control ($n = 10$) and Numb-cKO ($n = 9$) cells. (*E*) Control and Numb-cKO cerebellar slices were stimulated with 100 μM DHPG for 10 min, and mGlu1 in total and PSD fraction was immunoblotted 30 min or 180 min after DHPG challenge. GAPDH was the control. (*F*) Percentage changes of synaptic mGlu1 intensities were control: 100 ± 5% (0 min), 34 ± 4% (10 min + 30 min), 77 ± 8% (10 min + 180 min); cKO: 100 ± 4% (0 min), 96 ± 8% (10 min + 30 min), 103 ± 8% (10 min + 180 min). $n = 4$. *$P < 0.05$. **$P < 0.01$.

mGlu1 decreased to 34 ± 4% of the basal level at t = 40 min ($n = 4$; $P < 0.01$) but returned to 77 ± 8% at t = 190 min ($n = 4$; $P > 0.05$) (Fig. 5 *E* and *F*). The down- and up-regulation of mGlu1 expression in response to such agonist challenges was similar to results reported in previous work in other wild-type mice (66–68). In contrast, synaptic mGlu1 was not changed either 30 min or 180 min after DHPG application to Numb-cKO slices (t = 40 min: 96 ± 8%; t = 190 min: 103 ± 8%; $P > 0.05$ compared with baseline) (Fig. 5 *E* and *F*), suggesting that Numb is required for the internalization and recycling of mGlu1 in PCs.

Discussion

The present work reveals a previously unidentified role for Numb in cerebellar PCs: It regulates constitutive synaptic expression and dynamic trafficking of mGlu1 as well as LTD and motor coordination in young adult animals. Numb's functions in neurogenesis (7–10) and development (11, 12) have been reported previously, but to our knowledge this is the first report regarding Numb function in mature neurons. We showed that (*i*) Numb is expressed in PCs without coexpression of Numblike, (*ii*) deficiency of Numb does not overtly influence PC development, (*iii*) PC-specific Numb deficiency impairs motor coordination, (*iv*) Numb deficiency specifically decreases constitutive expression of synaptic mGlu1 in PCs and blocked induction of PF-LTD, and (*v*) the Numb-dependent decrease of mGlu1 currents is not caused by either deregulation of associated proteins or by short-term or long-term forms of mGlu1 plasticity but probably is caused mainly by aberrant internalization and recycling.

The putative role of Numb in internalization is supported by its possible role as an endocytic adaptor (13). Indeed, Numb contains PTB, PRR, DPF, and NPF motifs (2) and is located in clathrin-coated vesicles, probably functioning in the transport of a number of receptors (13). Prevailing evidence has shown that Numb exerts comparable roles in the development of neurons in culture (11, 12) and binds with β-amyloid precursor protein in neurodegenerative diseases (69). We report here that mGlu1 expression in the isolated synaptic fraction in Numb-cKO mice is reduced, although its total expression is not altered. Furthermore, mGlu1 EPSCs evoked by strong burst stimulation of PFs (38, 41, 42) are significantly decreased in Numb-cKO mice. Because mGlu1 is expressed primarily at perisynaptic sites adjacent and linked to the postsynaptic densities (PSDs) (70, 71), the present biochemical and electrophysiological data suggest a selective reduction of mGlu1 expression at the perisynaptic sites in PCs. In contrast, synaptic GluA2 in PCs was not affected by the ablation of Numb. Because Numb is an adaptor of clathrin complex, our findings lead to a hypothesis: Cargo selection during clathrin-dependent transportation is determined not by clathrin and its general adaptors, such as AP2, but by specified adaptor proteins, such as Numb.

In addition, we present several other important findings. We found that Numb is present in PCs, but Numblike is absent. This finding challenges the idea that Numb and Numblike generally coexist in neurons, as observed in neural stem cell studies (22). Possibly, this distinction also reflects a difference in developmental stage, because previously the roles of these proteins had not been investigated extensively in mature neurons. Furthermore, we found that development of spines and dendrites of PCs is largely normal in Numb-cKO mice. These findings place previous reports on the role of Numb in cultured neurons in a different light (11, 12). Possibly, the differences can be explained by differential effects under in vivo and in vitro conditions, but further experimentation is needed.

We show that both the constitutive expression and dynamic trafficking of mGlu1 are regulated by Numb. Evidence mainly from in vitro studies has shown that intracellular trafficking of mGlu1 is subjected to regulation by multiple signaling molecules. The internalization of mGlu1 may depend on various proteins, including arrestin and dynamin (72), protein kinase C (73), caveolar lipid rafts (64, 68), and Rab8 (66). Pandey et al. (67) found that recycling of mGlu1 depends on protein phosphatase 2A and Rab11. Thus, it will be interesting to determine whether and to what extent Numb-regulated internalization and recycling of mGlu1 are mediated by these molecules.

mGlu1 currents undergo STP and LTD in response to CF stimulation or PC depolarization (41, 61, 62), but the underlying mechanisms are not fully understood. Kim et al. (41) found that mGlu1-STP is blocked by depletion of IP_3-gated Ca^{2+} stores and postsynaptic IP_3R blockade, suggesting critical roles of endoplasmic reticulum. Kim et al. (61) hypothesized that mGlu1, $G\alpha_q$, or a protein that interacts with them is the molecular target of mGlu1-LTD. Here, we show that both mGlu1-STP and mGlu1-LTD remain intact, although the intracellular trafficking of mGlu1 is inhibited by Numb knockout. These findings suggest that stimulation protocols for mGlu1-STP and mGlu1-LTD do not induce dynamic transport of mGlu1 and that the plasticity of mGlu1 may be triggered by altered activity of mGlu1-associated proteins.

We found that Numb-cKO mice had impaired motor coordination, which may be directly ascribed to reduced mGlu1 currents, affecting PC excitability (30, 74). To what extent a deficit in mGlu1-dependent PF-LTD contributes to the phenotype on the accelerating rotarod remains to be determined. Many mouse mutants suffering from a lack of PF-LTD perform well on a rotarod, bringing into question a direct role of PF-LTD (17, 32). However, it is possible that a lack of PF-LTD in a motor learning process can be compensated by plastic inhibitory actions of molecular layer interneurons (33) and/or that the significance of PF-LTD and PF-LTP depends on the chemical identity of the modules involved (75, 76). Indeed, zebrin II^+ and zebrin II^- PCs show different intrinsic properties with probably different propensities for particular learning rules (77).

Materials and Methods

Animal experiments were carried out in accordance with the NIH *Guide for the Care and Use of Laboratory Animals* (78) and approved by the Animal Experimentation Ethics Committee of Zhejiang University. Mice in which exon 1 of the *Numb* gene was flanked by loxP sites were crossed with mice heterozygous for the L7-Cre transgene to obtain Numb-cKO mice. For all experimental details, see *SI Materials and Methods*. The primer sequences used for the SYBR Green probe (GenBank) are listed in Table S1. The riboprobe sequences are listed in Table S2.

ACKNOWLEDGMENTS. We thank Drs. Donggen Luo and Mengtong Li (Peking University) for confocal Ca^{2+} imaging, Dr. Xiaobing Yuan (Institute of Neuroscience, Chinese Academy of Sciences) for providing L7-Cre mice, and Dr. Richard Huganir (Johns Hopkins University) for kindly providing antibody. This work was supported by National Natural Science Foundation of China Grants 31471024, 31271148, 31200818, and 31571051; Natural Science Foundation of Zhejiang Province Grant Z15C090001; Shenzhen Committee for Technological Renovation Grant ZDSY20120617112838879; grants from the Dutch Organization for Medical Sciences (C.I.D.Z.) and Dutch Life Sciences (C.I.D.Z.); and European Research Council (ERC)-Advanced and ERC-Proof of Concept Grants (C.I.D.Z.).

1. Uemura T, Shepherd S, Ackerman L, Jan LY, Jan YN (1989) numb, a gene required in determination of cell fate during sensory organ formation in Drosophila embryos. *Cell* 58(2):349–360.
2. Gulino A, Di Marcotullio L, Screpanti I (2010) The multiple functions of Numb. *Exp Cell Res* 316(6):900–906.
3. Wakamatsu Y, Maynard TM, Jones SU, Weston JA (1999) NUMB localizes in the basal cortex of mitotic avian neuroepithelial cells and modulates neuronal differentiation by binding to NOTCH-1. *Neuron* 23(1):71–81.
4. Cayouette M, Raff M (2002) Asymmetric segregation of Numb: A mechanism for neural specification from Drosophila to mammals. *Nat Neurosci* 5(12): 1265–1269.
5. Zhong W, Jiang MM, Weinmaster G, Jan LY, Jan YN (1997) Differential expression of mammalian Numb, Numblike and Notch1 suggests distinct roles during mouse cortical neurogenesis. *Development* 124(10):1887–1897.
6. Johnson JE (2003) Numb and Numblike control cell number during vertebrate neurogenesis. *Trends Neurosci* 26(8):395–396.

7. Zhong W, et al. (2000) Mouse numb is an essential gene involved in cortical neurogenesis. *Proc Natl Acad Sci USA* 97(12):6844–6849.
8. Petersen PH, Zou K, Hwang JK, Jan YN, Zhong W (2002) Progenitor cell maintenance requires numb and numblike during mouse neurogenesis. *Nature* 419(6910):929–934.
9. Petersen PH, Zou K, Krauss S, Zhong W (2004) Continuing role for mouse Numb and Numbl in maintaining progenitor cells during cortical neurogenesis. *Nat Neurosci* 7(8):803–811.
10. Rasin MR, et al. (2007) Numb and Numbl are required for maintenance of cadherin-based adhesion and polarity of neural progenitors. *Nat Neurosci* 10(7):819–827.
11. Nishimura T, et al. (2006) Role of numb in dendritic spine development with a Cdc42 GEF intersectin and EphB2. *Mol Biol Cell* 17(3):1273–1285.
12. Nishimura T, et al. (2003) CRMP-2 regulates polarized Numb-mediated endocytosis for axon growth. *Nat Cell Biol* 5(9):819–826.
13. Santolini E, et al. (2000) Numb is an endocytic protein. *J Cell Biol* 151(6):1345–1352.
14. Wang YT, Linden DJ (2000) Expression of cerebellar long-term depression requires postsynaptic clathrin-mediated endocytosis. *Neuron* 25(3):635–647.
15. Aiba A, et al. (1994) Deficient cerebellar long-term depression and impaired motor learning in mGluR1 mutant mice. *Cell* 79(2):377–388.
16. Schonewille M, et al. (2010) Purkinje cell-specific knockout of the protein phosphatase PP2B impairs potentiation and cerebellar motor learning. *Neuron* 67(4):618–628.
17. Schonewille M, et al. (2011) Reevaluating the role of LTD in cerebellar motor learning. *Neuron* 70(1):43–50.
18. Linden DJ (2003) Neuroscience. From molecules to memory in the cerebellum. *Science* 301(5640):1682–1685.
19. Hartmann J, et al. (2004) Distinct roles of Galpha(q) and Galpha11 for Purkinje cell signaling and motor behavior. *J Neurosci* 24(22):5119–5130.
20. Wu ZY, et al. (2012) AMPA receptors regulate exocytosis and insulin release in pancreatic β cells. *Traffic* 13(8):1124–1139.
21. Ji YF, et al. (2013) Upregulation of glutamate transporter GLT-1 by mTOR-Akt-NF-κB cascade in astrocytic oxygen-glucose deprivation. *Glia* 61(12):1959–1975.
22. Kuo CT, et al. (2006) Postnatal deletion of Numb/Numblike reveals repair and remodeling capacity in the subventricular neurogenic niche. *Cell* 127(6):1253–1264.
23. Barski JJ, Dethleffsen K, Meyer M (2000) Cre recombinase expression in cerebellar Purkinje cells. *Genesis* 28(3-4):93–98.
24. Klein AL, Zilian O, Suter U, Taylor V (2004) Murine numb regulates granule cell maturation in the cerebellum. *Dev Biol* 266(1):161–177.
25. Dehnes Y, et al. (1998) The glutamate transporter EAAT4 in rat cerebellar Purkinje cells: A glutamate-gated chloride channel concentrated near the synapse in parts of the dendritic membrane facing astroglia. *J Neurosci* 18(10):3606–3619.
26. Le TD, et al. (2010) Lipid signaling in cytosolic phospholipase $A_2\alpha$-cyclooxygenase-2 cascade mediates cerebellar long-term depression and motor learning. *Proc Natl Acad Sci USA* 107(7):3198–3203.
27. Ohtani Y, et al. (2014) The synaptic targeting of mGluR1 by its carboxyl-terminal domain is crucial for cerebellar function. *J Neurosci* 34(7):2702–2712.
28. Ito M, Kano M (1982) Long-lasting depression of parallel fiber-Purkinje cell transmission induced by conjunctive stimulation of parallel fibers and climbing fibers in the cerebellar cortex. *Neurosci Lett* 33(3):253–258.
29. Miyata M, Okada D, Hashimoto K, Kano M, Ito M (1999) Corticotropin-releasing factor plays a permissive role in cerebellar long-term depression. *Neuron* 22(4):763–775.
30. Ichise T, et al. (2000) mGluR1 in cerebellar Purkinje cells essential for long-term depression, synapse elimination, and motor coordination. *Science* 288(5472):1832–1835.
31. Goossens J, et al. (2001) Expression of protein kinase C inhibitor blocks cerebellar long-term depression without affecting Purkinje cell excitability in alert mice. *J Neurosci* 21(15):5813–5823.
32. De Zeeuw CI, et al. (2011) Spatiotemporal firing patterns in the cerebellum. *Nat Rev Neurosci* 12(6):327–344.
33. Gao Z, van Beugen BJ, De Zeeuw CI (2012) Distributed synergistic plasticity and cerebellar learning. *Nat Rev Neurosci* 13(9):619–635.
34. Ly R, et al. (2013) T-type channel blockade impairs long-term potentiation at the parallel fiber-Purkinje cell synapse and cerebellar learning. *Proc Natl Acad Sci USA* 110(50):20302–20307.
35. Lev-Ram V, Wong ST, Storm DR, Tsien RY (2002) A new form of cerebellar long-term potentiation is postsynaptic and depends on nitric oxide but not cAMP. *Proc Natl Acad Sci USA* 99(12):8389–8393.
36. Belmeguenai A, Hansel C (2005) A role for protein phosphatases 1, 2A, and 2B in cerebellar long-term potentiation. *J Neurosci* 25(46):10768–10772.
37. Wang DJ, et al. (2014) Long-term potentiation at cerebellar parallel fiber-Purkinje cell synapses requires presynaptic and postsynaptic signaling cascades. *J Neurosci* 34(6):2355–2364.
38. Brasnjo G, Otis TS (2001) Neuronal glutamate transporters control activation of postsynaptic metabotropic glutamate receptors and influence cerebellar long-term depression. *Neuron* 31(4):607–616.
39. Ito M (2006) Cerebellar circuitry as a neuronal machine. *Prog Neurobiol* 78(3-5):272–303.
40. Shigemoto R, Nakanishi S, Mizuno N (1992) Distribution of the mRNA for a metabotropic glutamate receptor (mGluR1) in the central nervous system: An in situ hybridization study in adult and developing rat. *J Comp Neurol* 322(1):121–135.
41. Kim SJ, et al. (2008) Transient upregulation of postsynaptic IP3-gated Ca release underlies short-term potentiation of metabotropic glutamate receptor 1 signaling in cerebellar Purkinje cells. *J Neurosci* 28(17):4350–4355.
42. Su LD, Sun CL, Shen Y (2010) Ethanol acutely modulates mGluR1-dependent long-term depression in cerebellum. *Alcohol Clin Exp Res* 34(7):1140–1145.
43. Sun CL, Su LD, Li Q, Wang XX, Shen Y (2011) Cerebellar long-term depression is deficient in Niemann-Pick type C disease mice. *Cerebellum* 10(1):88–95.
44. Safo PK, Regehr WG (2005) Endocannabinoids control the induction of cerebellar LTD. *Neuron* 48(4):647–659.
45. Han VZ, Zhang Y, Bell CC, Hansel C (2007) Synaptic plasticity and calcium signaling in Purkinje cells of the central cerebellar lobes of mormyrid fish. *J Neurosci* 27(49):13499–13512.
46. Uesaka N, Kawata S, Kano M (2014) Cellular and molecular mechanisms of synapse elimination in the Mammalian brain. *Brain Nerve* 66(9):1069–1077.
47. Kreitzer AC, Regehr WG (2001) Retrograde inhibition of presynaptic calcium influx by endogenous cannabinoids at excitatory synapses onto Purkinje cells. *Neuron* 29(3):717–727.
48. Tanimura A, Kawata S, Hashimoto K, Kano M (2009) Not glutamate but endocannabinoids mediate retrograde suppression of cerebellar parallel fiber to Purkinje cell synaptic transmission in young adult rodents. *Neuropharmacology* 57(2):157–163.
49. Wang DJ, et al. (2012) Cytosolic phospholipase A2 alpha/arachidonic acid signaling mediates depolarization-induced suppression of excitation in the cerebellum. *PLoS One* 7(8):e41499.
50. Ohno-Shosaku T, Kano M (2014) Endocannabinoid-mediated retrograde modulation of synaptic transmission. *Curr Opin Neurobiol* 29:1–8.
51. Maejima T, Hashimoto K, Yoshida T, Aiba A, Kano M (2001) Presynaptic inhibition caused by retrograde signal from metabotropic glutamate to cannabinoid receptors. *Neuron* 31(3):463–475.
52. Brown SP, Brenowitz SD, Regehr WG (2003) Brief presynaptic bursts evoke synapse-specific retrograde inhibition mediated by endogenous cannabinoids. *Nat Neurosci* 6(10):1048–1057.
53. Kano M, et al. (1995) Impaired synapse elimination during cerebellar development in PKC gamma mutant mice. *Cell* 83(7):1223–1231.
54. Finch EA, Augustine GJ (1998) Local calcium signalling by inositol-1,4,5-trisphosphate in Purkinje cell dendrites. *Nature* 396(6713):753–756.
55. Canepari M, Ogden D (2006) Kinetic, pharmacological and activity-dependent separation of two Ca^{2+} signalling pathways mediated by type 1 metabotropic glutamate receptors in rat Purkinje neurones. *J Physiol* 573(Pt 1):65–82.
56. Hartmann J, et al. (2008) TRPC3 channels are required for synaptic transmission and motor coordination. *Neuron* 59(3):392–398.
57. Chae HG, et al. (2012) Transient receptor potential canonical channels regulate the induction of cerebellar long-term depression. *J Neurosci* 32(37):12909–12914.
58. Hartmann J, et al. (2014) STIM1 controls neuronal Ca^{2+} signaling, mGluR1-dependent synaptic transmission, and cerebellar motor behavior. *Neuron* 82(3):635–644.
59. Roche KW, et al. (1999) Homer 1b regulates the trafficking of group I metabotropic glutamate receptors. *J Biol Chem* 274(36):25953–25957.
60. Karim F, Wang CC, Gereau RW, 4th (2001) Metabotropic glutamate receptor subtypes 1 and 5 are activators of extracellular signal-regulated kinase signaling required for inflammatory pain in mice. *J Neurosci* 21(11):3771–3779.
61. Jin Y, Kim SJ, Kim J, Worley PF, Linden DJ (2007) Long-term depression of mGluR1 signaling. *Neuron* 55(2):277–287.
62. Batchelor AM, Garthwaite J (1997) Frequency detection and temporally dispersed synaptic signal association through a metabotropic glutamate receptor pathway. *Nature* 385(6611):74–77.
63. Dhami GK, Ferguson SS (2006) Regulation of metabotropic glutamate receptor signaling, desensitization and endocytosis. *Pharmacol Ther* 111(1):260–271.
64. Francesconi A, Kumari R, Zukin RS (2009) Regulation of group I metabotropic glutamate receptor trafficking and signaling by the caveolar/lipid raft pathway. *J Neurosci* 29(11):3590–3602.
65. Choi KY, Chung S, Roche KW (2011) Differential binding of calmodulin to group I metabotropic glutamate receptors regulates receptor trafficking and signaling. *J Neurosci* 31(16):5921–5930.
66. Esseltine JL, Ribeiro FM, Ferguson SS (2012) Rab8 modulates metabotropic glutamate receptor subtype 1 intracellular trafficking and signaling in a protein kinase C-dependent manner. *J Neurosci* 32(47):16933–42a.
67. Pandey S, Mahato PK, Bhattacharyya S (2014) Metabotropic glutamate receptor 1 recycles to the cell surface in protein phosphatase 2A-dependent manner in non-neuronal and neuronal cell lines. *J Neurochem* 131(5):602–614.
68. Hong YH, et al. (2009) Agonist-induced internalization of mGluR1alpha is mediated by caveolin. *J Neurochem* 111(1):61–71.
69. Roncarati R, et al. (2002) The gamma-secretase-generated intracellular domain of beta-amyloid precursor protein binds Numb and inhibits Notch signaling. *Proc Natl Acad Sci USA* 99(10):7102–7107.
70. Scannevin RH, Huganir RL (2000) Postsynaptic organization and regulation of excitatory synapses. *Nat Rev Neurosci* 1(2):133–141.
71. Sheng M, Kim MJ (2002) Postsynaptic signaling and plasticity mechanisms. *Science* 298(5594):776–780.
72. Mundell SJ, Matharu AL, Pula G, Roberts PJ, Kelly E (2001) Agonist-induced internalization of the metabotropic glutamate receptor 1a is arrestin- and dynamin-dependent. *J Neurochem* 78(3):546–551.
73. Mundell SJ, Pula G, Carswell K, Roberts PJ, Kelly E (2003) Agonist-induced internalization of metabotropic glutamate receptor 1A: Structural determinants for protein kinase C- and G protein-coupled receptor kinase-mediated internalization. *J Neurochem* 84(2):294–304.
74. Coesmans M, et al. (2003) Mechanisms underlying cerebellar motor deficits due to mGluR1-autoantibodies. *Ann Neurol* 53(3):325–336.
75. Wadiche JI, Jahr CE (2005) Patterned expression of Purkinje cell glutamate transporters controls synaptic plasticity. *Nat Neurosci* 8(10):1329–1334.
76. Ebner TJ, Wang X, Gao W, Cramer SW, Chen G (2012) Parasagittal zones in the cerebellar cortex differ in excitability, information processing, and synaptic plasticity. *Cerebellum* 11(2):418–419.
77. Zhou H, et al. (2014) Cerebellar modules operate at different frequencies. *eLife* 3:e02536.
78. Committee on Care and Use of Laboratory Animals (1996) Guide for the Care and Use of Laboratory Animals (Natl Inst Health, Bethesda), DHHS Publ No (NIH) 85-23.
79. Lee KJ, Kim H, Kim TS, Park SH, Rhyu IJ (2004) Morphological analysis of spine shapes of Purkinje cell dendrites in the rat cerebellum using high-voltage electron microscopy. *Neurosci Lett* 359(1-2):21–24.
80. Dai ZM, et al. (2014) Stage-specific regulation of oligodendrocyte development by Wnt/β-catenin signaling. *J Neurosci* 34(25):8467–8473.